JNTM JOURNAL of NEW TECHNOLOGY and MATERIALS

Journal of New Technology and Materials

Vol. 15, No. 2 (2025), 10–23

RESEARCH ARTICLE

Thermokinetic Substrate-Lattice Prioritization of Engineered *Thermus thermophilus* α-oxoamine synthase Variants for SNAc-Enabled Aminoketone and Pyrrole Synthesis

T. Layne[1,*], W. Kim[2] and J. E. Greene[2]

[1]Department of Materials Science and Engineering, Yonsei University, 50 Yonsei-ro, Seodaemun-gu, Seoul 03722, Republic of Korea. [2]Materials Research Laboratory and Materials Science Department, University of Illinois, 104 South Goodwin, Urbana, Illinois 61801

*Correspondence: layne29@@yonsei.ac.kr

Received date: March 11, 2025; Accepted date: October 12, 2025

Abstract

In the current research paper, the following process-design problem is considered: can the activity, thermostability and simplified thioester data obtained for the designed V79 variants of the engineered *Thermus thermophilus* α-oxoamine synthase be converted into a repeatable selection process for the catalysts used in aminoketone and pyrrole synthesis? To address this challenge, thermokinetic substrate-lattice prioritization, a route-selection procedure, which distinguishes between discovery potential and preparative capacity, is developed. Unlike a routine set of enzymatic screening assays, the current data set represents the V79 variant matrix characterized by amino acid acceptance, acyl-CoA donor range, residual activity after 70 and 90 °C thermal stress, acetyl-SNAc resistance and the glycine/acetyl-SNAc/methyl acetoacetate pyrrole synthesis pathway. In this approach, the observable activity is presented as a substrate-lattice function and merged with normalized heat stability, acyl donor tolerance and SNAc-based route efficiency metrics. The resulting selection process produces a non-redundant ranking: V79G variant is recommended for exploration of novel amino acids and hydrophobic acyl donor routes, while V79S should be employed in propargyl and selected aromatic acyl donors route development. Finally, V79A variant is recommended for preparative SNAc-based pyrrole synthesis due to its broad amino acid range, best severe temperature stability among all active engineered mutants and 35% analytical pyrrole yield achieved at 60 °C.

Keywords: α-oxoamine synthase, pyridoxal phosphate, thermostable enzyme, N-acetylcysteamine thioester, aminoketone, pyrrole, route selection, materials chemistry

1 Introduction

Selective carbon-carbon bond formation is key in the preparation of fine chemicals, pharmaceutical intermediates, ligands, chromophores, monomer precursors and heteroatom-rich molecules. While many conventional methods for C–C bond formation continue to be effective, they tend to require strong bases, organometallic reagents, stoichiometric additives or protection/deprotection cycles. Biocatalysis complements traditional catalysis because enzymes form bonds under milder conditions and maintain excellent chemoselectivity, regioselectivity and stereoselectivity. Biocatalysis is relevant to sustainable chemistry because of advances in green metrics, enzyme engineering and biocatalytic synthetic processes [1–3]. The final open issue in such projects involves the conversion of screening results into a process chemist's decision about catalyst, donor, substrate type and temperature.

The recent literature in biocatalysis moves beyond isolated experiments showing enzyme catalysis toward the construction of retrosynthetic disconnections. Enzymes have been rendered versatile enough by directed evolution and rational

mutagenesis for non-native catalysis. Industrial applications of biocatalysis have confirmed the need to consider multiple criteria (substrate loading, thermal stability, catalytic medium, cofactor economy and product recovery) when selecting an enzyme for a reaction [4–6]. Protein engineering allows enzymes to catalyse reactions outside metabolic contexts, and directed evolution and structure-based repurposing reveal how single substitutions produce new catalytic capabilities [7, 8]. Nonetheless, it is unlikely that a protein variant will maximize all criteria at once. Variants with large pockets gain in substrate tolerance but become less stable; substitutions producing novel interaction motifs improve recognition without increasing catalytic breadth; and good results in microscale screens are no guarantee of the best preparative catalyst. All such considerations argue for decision models keeping activity, stability and economy as independent terms [9, 10].

Biocatalytic retrosynthetic approaches have also contributed to interpretation of biocatalytic results. Biocatalytic retrosynthesis is concerned with determining whether an enzymatic disconnection shortens a chemical route, increases its selectivity or yields an intermediate not easily accessed by conventional means [11–13]. Cascade systems highlight another essential point – that route efficiency is determined by the compatibility of sequential enzyme-mediated and chemical steps [14, 15]. This aspect becomes critical in material-relevant synthesis because the focus is often less on amino-acid-based biologicals and more on aminoketone-functionalized heterocycles. It follows that biocatalytic screens have to determine not just which enzyme works best but which one is best for particular stages of synthesis.

Enzymes that use the pyridoxal 5'-phosphate (PLP) cofactor represent a good case for this approach. PLP is well known as a stabilizer of carbanionic species, and, through an internal-aldimine/external-aldimine transition, it catalyzes reactions at the α-carbon of amino-acid substrates. The subsequent stereoelectronic effect dictates what kind of chemistry is promoted: transamination, decarboxylation, racemization, elimination or C–C bond formation [16–18]. The structural and evolutionary research has confirmed that PLP cofactor can drive different classes of reactions, depending on substrate-protein contacts, hydrogen-bonding pattern and active-site architecture [19–21]. This enzyme versatility is valuable but it adds complexity to activity ranking because a single active-site modification affects enzyme activity, substrate binding and even thermal stability.

A specific class of PLP enzymes worth mentioning are the α-oxoamine synthases (AOS). A characteristic feature of AOS members is that they catalyze irreversible, decarboxylative Claisen-type condensation between amino acids and acyl-thioesters, forming aminoketones as products. This group of compounds represents an interesting target for biocatalysis because aminoketones can be converted into pyrroles and other structures, illustrating a larger biosynthetic principle of generating diversity using modular enzyme chemistry [22]. AOS enzymes occur in pathways of heme, biotin and sphingolipid biosynthesis. The crystallography and site-directed mutagenesis studies of 5-aminolevulinate synthase, 8-amino-7-oxononanoate synthase and serine palmitoyltransferase have revealed mechanisms of PLP binding, acyl-thioester recognition and conformational change [23–25]. Additionally, inhibition studies have shown that small substitutions near the PLP moiety influence the activity against both amino acids and thioesters [26]. This enzyme family represents a promising but challenging system for catalyzing C–C bond formation.

There are two practical reasons preventing AOS enzymes from being widely adopted in synthetic routes. One is that the natural substrates of many AOS enzymes include few metabolic members. Another problem is associated with the expense and operational complexity of natural acyl-CoA donors used in biocatalysis. Simplified N-acetylcysteamine (SNAc) thioesters could be a solution because they lack bulky CoA units but maintain a thioester motif. Previous experience with thermostable AOSs has confirmed that the combination of PLP-driven irreversible amine ketone formation and subsequent Knorr-type pyrrole closure is highly efficient [27–29]. Thus, the next task to tackle becomes clear: How should the matrix of *Thermus thermophilus* α-oxoamine synthase variants at V79 be interpreted in light of the route design rather than mere activity search?

The *Thermus thermophilus* α-oxoamine synthase variants used in this work belong to a particular series of mutants where the residue V79 was replaced by Gln, Ala, Gly, Ser or Leu. Residue V79 is situated close to the PLP binding site and interacts with amino acids to control the formation of an appropriate pocket that holds the external aldimine formed by PLP and incoming acyl donor. V79 substitutions (Gln, Ala, Gly, Ser or Leu) produce differences in pocket depth and local charge distribution that change enzyme specificity and affinity. The current study uses the following information from *Thermus thermophilus* α-oxoamine synthase variant matrix as screening parameters: breadth of amino-acid acceptors, catalytic efficiency, broadening of acyl-CoA scope, heat resistance at 70 and 90 °C, ability to use SNAc donors and yield of pyrrole 1 in SNAc-driven Knorr reaction. Each parameter measures something different: Breadth measures discoverability of new substrates; resistance measures stability; acyl-donor breadth determines applicability to a wide variety of pyrroles; SNAc ability measures feasibility of cost-effective synthesis.

The research question posed in this work is: *Can the Thermus thermophilus α-oxoamine synthase V79 matrix of engineered mutants be transformed into a route-selection map assigning specific roles to the main mutants in materials-relevant aminoketone and pyrrole synthesis?* Unlike in a generic enzyme engineering study where it is asked which variant gives highest activity in screens, the present work seeks to establish whether a thermokinetic/substrate-lattice model could distinguish suitable catalysts for a specific task. Based on the data collected in this work, the answer is positive. thermokinetic substrate-lattice prioritization indicates that three major V79 mutants (V79G, V79S and V79A) should be assigned distinct roles.

Table 1 is included to prevent the paper from becoming a generic summary of biocatalysis. It fixes the research question,

dataset, method, result and conclusion around one internally consistent task. The rest of the manuscript expands each component: the methodology defines how the lattice is encoded, and the Results and Discussion section explains why each figure and table changes the catalyst recommendation.

Table 1. Unique characteristics of the present paper as a route-selection study.

Component	Paper-specific definition
Research question	Can the *Thermus thermophilus* α-oxoamine synthase V79 variant matrix be converted into a catalyst-route map for aminoketone and pyrrole synthesis?
Dataset	*Thermus thermophilus* α-oxoamine synthase V79 matrix: amino-acid acceptor breadth, acyl-CoA reach, residual activity 70/90 °C, SNAc compatibility and yield of pyrrole 1.
Method	Thermokinetic/substrate-lattice prioritization with activity encoding, heat persistence normalization, acyl-donor elasticity and SNAc-cascade feasibility.
Result	V79G, V79S and V79A assigned to aminoketone discovery, functional handle mapping, aryl pyrrole formation.
Conclusion	Catalyst suitability depends on goal; preparative catalyst chosen based on thermal intersection of substrate breadth and SNAc economy.

2 Experimental Basis and Process-Selection Framework

2.1 Data Source, Input Fields, and Model Boundaries

The process-selection model was constructed from the *Thermus thermophilus* α-oxoamine synthase V79 engineering data reported by Ashley and co-workers [30]. The retained inputs were selected because they directly influence route design: amino-acid activity with acetyl-CoA, acyl-CoA chain-length compatibility, residual activity after 70 and 90 °C heat treatments, acetyl-SNAc activity, and pyrrole-cascade performance. The model does not reinterpret heat-map colors as exact kinetic constants. It uses detectable activity, accepted amino-acid classes, residual-activity values, and the reported 35% analytical yield for pyrrole formation from glycine, acetyl-SNAc, and methyl acetoacetate with V79A at 60 °C.

Table 2. Experimental fields used to construct the thermokinetic substrate-lattice model.

Model field	Quantitative or categorical input used for route selection
Amino-acid breadth	33 amino acids were considered in the acetyl-CoA screen; V79A and V79G were active with 16 amino acids, including seven proteinogenic amino acids and nine unnatural amino acids.
Kinetic improvement window	V79A improved catalytic efficiency by 2.4–64.8-fold for the four reference amino-acid reactions; V79G improved by 2.7–57.5-fold and generally showed faster behaviour in the same subset.
Acyl-donor elasticity	V79G, V79A and V79S retained activity across C2–C8 acyl-CoA donors; V79G extended to C10 and C12 donors, while V79S uniquely supported L-Pra condensation with C2–C8 acyl-CoA donors.
Thermal persistence	After 2 h at 70 °C, WT, V79L, V79A, V79S and V79G retained 89%, 92%, 78%, 79% and 56% activity, respectively; after 120 min at 90 °C, V79A retained about 60%, V79S about 45%, WT about 15%, and V79G/V79L about 5% or less.
SNAc cascade utility	V79A generated pyrrole 1 from Gly, acetyl-SNAc and methyl acetoacetate in 35% analytical yield at 60 °C; increasing acetyl-SNAc loading from 32 to 800 mM did not substantially improve yield.

Table 2 defines the dataset used in the paper. Its importance is methodological: the entries are deliberately heterogeneous because catalyst selection is heterogeneous. A variant that is broad in amino-acid scope may still be unsuitable for a thermally demanding SNAc cascade, and a thermally persistent variant may still be unattractive if it cannot accept the desired donor. The model therefore treats each row as a separate decision layer before integrating them into a final process-readiness score.

2.2 Structural Context for Variant-Level Route Selection

The structural basis for separating substrate breadth from process readiness is shown in Figures 1, 2 and 3. PLP remains the central catalytic organizer, but residue 79 modulates the region in which the amino-acid side chain and acyl-thioester partner must be accommodated. These figures justify the use of separate lattice terms: an alanine substitution does not create the same chemical environment as glycine or serine, and the route consequence is therefore not reducible to a single mutant label.

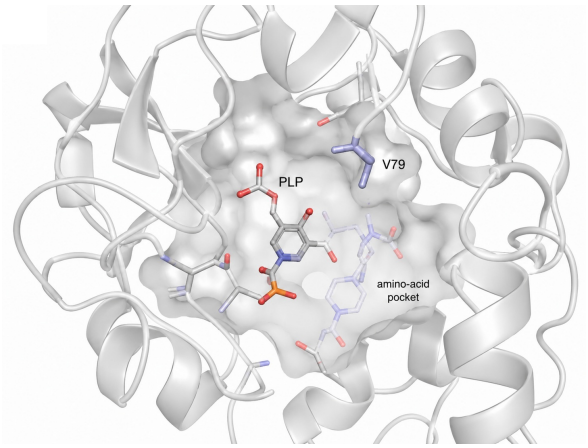

Figure 1. Active-site context of *Thermus thermophilus* α-oxoamine synthase used for thermokinetic substrate-lattice interpretation. PLP occupies the central catalytic pocket, residue V79 is located near the amino-acid recognition region, and the surrounding protein surface defines the accessible volume for external-aldimine and acyl-thioester approach.

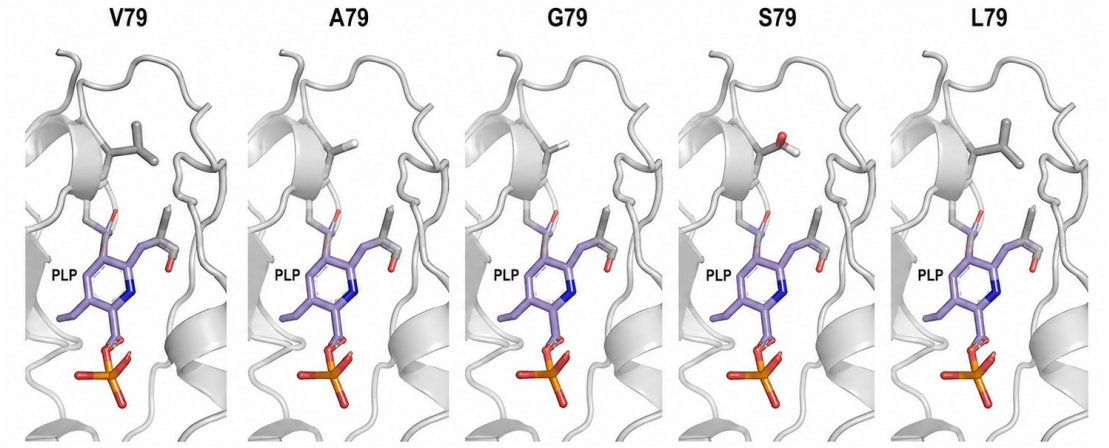

Figure 2. Loop-level comparison of the residue-79 variants considered in the TSLP ranking. The V79, A79, G79, S79 and L79 views show how side-chain size and polarity alter the local environment around PLP while preserving the overall fold.

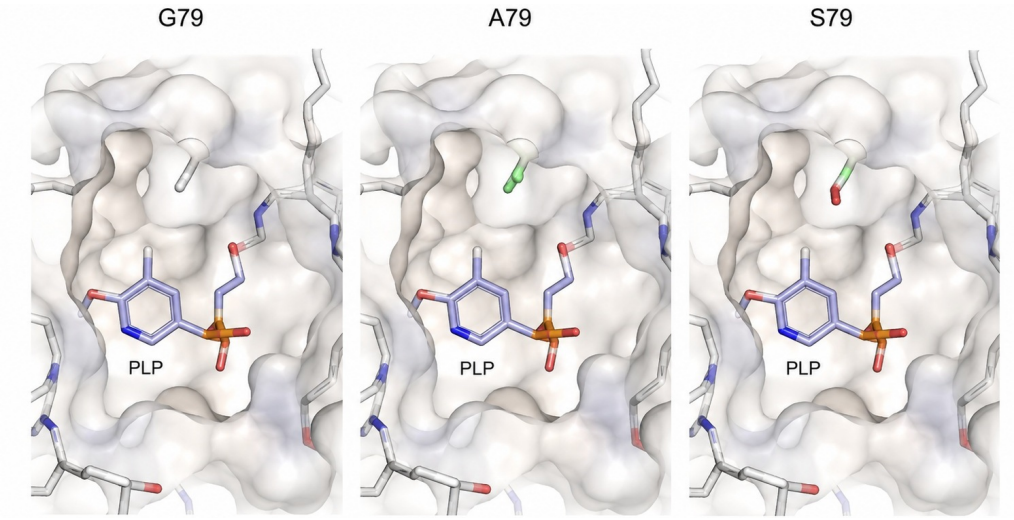

Figure 3. Surface-pocket comparison for G79, A79 and S79. The G79 cavity provides the most open amino-acid entry region, A79 preserves a compact methyl contact that supports thermal resilience, and S79 introduces a polar side chain that can favour selected functional-handle combinations.

Figures 1–3 also establish a mechanistic caution for the scoring model. Pocket opening is helpful for exploratory substrate acceptance, but excessive local flexibility can reduce heat resistance. Conversely, a compact substitution may not maximize screening speed but can preserve the local packing required for elevated-temperature synthesis. This explains why the method does not use amino-acid breadth alone as the final decision criterion.

2.3 Activity Encoding and Amino-Acid Breadth Metric

For a variant v and substrate entry s, the activity state was encoded as

$$A_{v,s} = \begin{cases} 1, & \text{detectable activity for the variant–substrate pair,} \\ 0, & \text{no detectable activity for the variant–substrate pair.} \end{cases} \tag{1}$$

Eq. (1) converts qualitative screening entries into a reproducible binary substrate lattice. The equation does not claim that all positive entries are kinetically equivalent; instead, it identifies the minimum route-design fact that a combination is experimentally viable under the tested conditions. This interpretation prevents overfitting of a semi-quantitative screen while still retaining the information needed for first-pass catalyst selection.

The amino-acid breadth term for each variant was calculated as

$$B_v = \frac{1}{N_{AA}} \sum_{s=1}^{N_{AA}} A_{v,s}, \tag{2}$$

where N_{AA} is the number of amino-acid entries in the screen. Eq. (2) measures coverage rather than speed. For example, 16 active amino acids among 33 tested entries indicates a broad discovery envelope, but it does not automatically identify the best preparative catalyst. This distinction is essential because preparative synthesis also requires thermal persistence, donor economy, and cascade compatibility.

2.4 Thermal Persistence and Acyl-Donor Elasticity Metrics

The normalized thermal persistence term was defined as

$$H_v = 0.40 \left(\frac{R_{70,v}}{R_{70,\max}} \right) + 0.60 \left(\frac{R_{90,v}}{R_{90,\max}} \right), \tag{3}$$

where $R_{70,v}$ and $R_{90,v}$ are residual activities after heat treatment at 70 and 90 °C, respectively. Eq. (3) gives greater weight to the 90 °C field because severe heating differentiates variants that might otherwise appear similar at 70 °C. A variant that remains active after moderate heating may still be unsuitable for a robust cascade if it collapses under harsher thermal stress. The equation therefore represents process resilience, not merely protein survival.

The acyl-donor elasticity term was expressed as

$$E_v = 0.60 C_v + 0.25 L_v + 0.15 Aryl_v, \tag{4}$$

where C_v represents short-to-medium chain coverage, L_v represents long-chain extension, and $Aryl_v$ represents detectable benzoyl-CoA compatibility. Eq. (4) recognizes that acyl-donor scope is not a single property. C2–C8 coverage supports general aminoketone route development, C10–C12 activity expands access to hydrophobic products, and aryl donor compatibility opens routes to aromatic aminoketone derivatives. The weighting keeps C2–C8 coverage dominant because those donors define the broadest practical design space in the available matrix.

2.5 Integrated Process-Readiness Score and Route-Prioritization Workflow

The final process-readiness score was calculated as

$$P_v = 100 \left(0.30 B_v + 0.30 H_v + 0.20 E_v + 0.20 S_v \right), \tag{5}$$

where S_v is the SNAc-route compatibility term. Eq. (5) deliberately avoids ranking variants only by substrate breadth. Breadth and thermal persistence receive equal weight because the intended application is not only the discovery of active substrate combinations but the selection of variants for thermally robust synthesis. The SNAc term is included because replacement of acyl-CoA donors with cysteamine-derived thioesters changes the economic feasibility of preparative synthesis. The score is a route-selection aid rather than a universal kinetic descriptor.

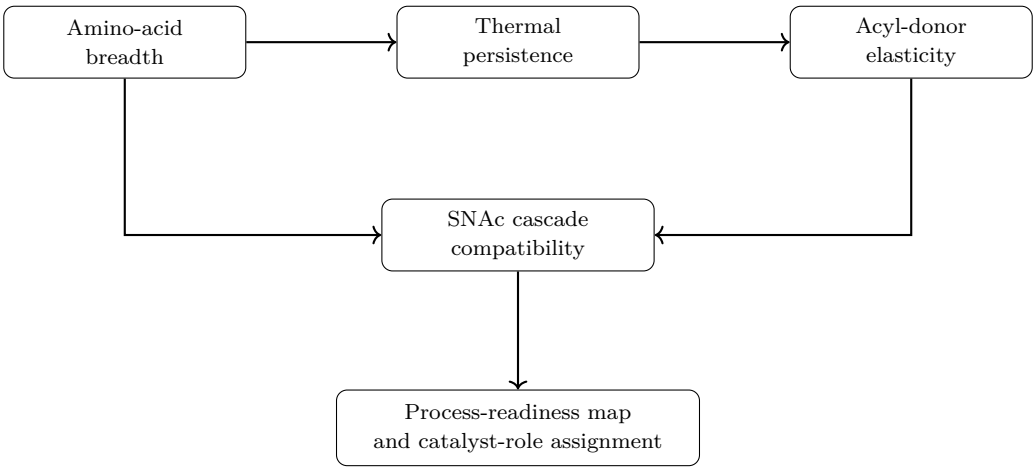

Figure 4. Thermokinetic substrate-lattice prioritization workflow used to assign *Thermus thermophilus* α-oxoamine synthase V79 variants to practical synthetic roles. The model integrates activity breadth, heat resistance, acyl-donor compatibility and SNAc cascade behaviour before making a route recommendation.

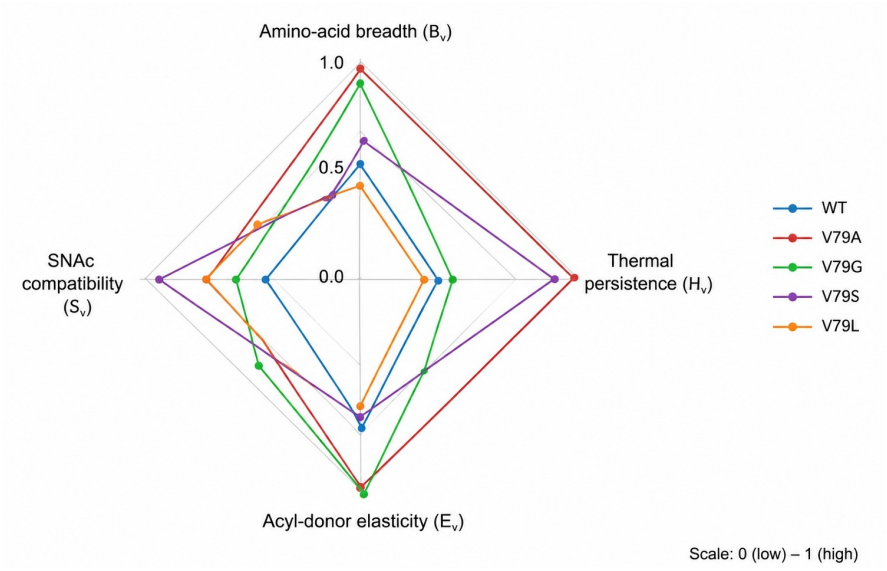

Figure 5. Normalized TSLP radar decision map for WT, V79A, V79G, V79S and V79L. The axes compare amino-acid breadth, thermal persistence, acyl-donor elasticity and SNAc compatibility on a 0–1 scale.

Figures 4 and 5 show how the equations function together. The workflow figure is the logical sequence: information is separated into four fields before the final route assignment. The radar map is the visual audit of the same reasoning: V79A occupies the most balanced preparative region, V79G expands breadth and donor reach, and V79S forms a distinct functional-handle region. The figure therefore checks that the process score is not being driven by a single axis.

3 Results and Discussion

3.1 Answer to the research question

The question posed at the outset was whether the V79 data could be translated into a route-selection map rather than a single ranking of activities. The answer is yes, but only with respect to synthetic objective. The same matrix provides

three possible solutions: use V79G for the discovery of amino acid and acyl-donor combinations; use V79S for access to propargyl or selected aryl-acyl aminoketones; and use V79A for construction of a simplified, thermally assisted SNAc route to pyrrole 1. This point is fundamental to the paper's conclusions.

It implies that there is no such thing as the best enzyme. Rather, V79G is best suited to searches, V79S is best suited to mapping, and V79A is best suited to construction. It also implies that a typical overstatement in many enzyme-engineering papers must be avoided. Specifically, the variant that demonstrates most broad screening behavior or that screens fastest should not automatically become a candidate for the temperature-stress thioester cascade.

3.2 Amino-acid breadth distinguishes between discovery and synthesis

The amino-acid level of interpretation singles out V79A and V79G as the two most broadly reactive mutants because both accept 16 of the 33 amino acids screened in the acetyl-CoA assay. The two groups are not only numerically broad, but they are also chemically diverse. They comprise not only the proteinogenic amino acids L-Ala, L-Asp, Gly, L-Ile, L-Ser, L-Thr and L-Val, but also the unnatural amino acids L-Aba, DL-Alg, L-Cpa, L-Cpg, L-Hsr, α-Ile, L-Nva, L-Pra and L-Oas. This breadth is significant for the reasons stated below.

The breadth term can be explained structurally with regard to Figure 6, which depicts the proteinogenic subset and Figure 7, which depicts the unnatural subset. With respect to the former, we can see that the redesigned active site is tolerant to small, branched, and even polar amino acids. The latter subset carries more weight with respect to route planning because it includes amino acids with an alkyne, cycloalkyl, hydroxy or sulfone side chain.

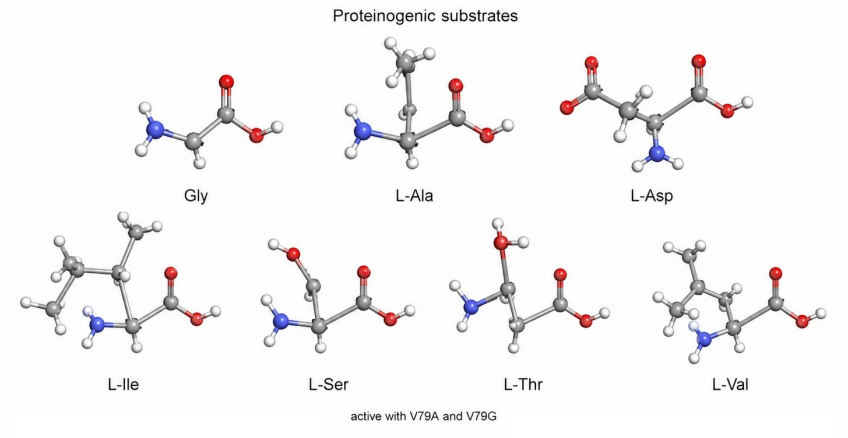

Figure 6. Proteinogenic amino-acid substrates accepted by the engineered V79 variants. Gly, L-Ala, L-Asp, L-Ile, L-Ser, L-Thr and L-Val define the natural-substrate region of the lattice and establish that V79A and V79G maintain access to chemically varied amino-acid classes.

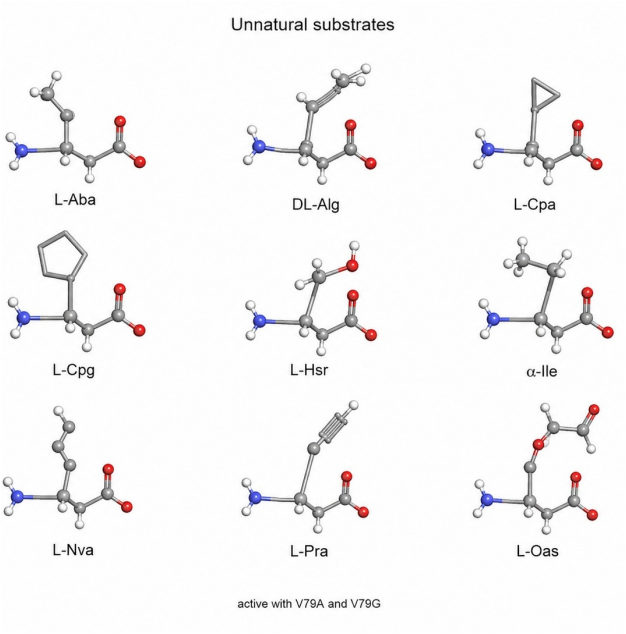

Figure 7. Unnatural amino-acid substrates accepted by V79A and V79G. The accepted entries include alkyl, alkenyl, alkyne, cyclopropyl, cyclopentyl, hydroxy and sulfone-containing side chains, demonstrating that residue-79 engineering broadens the chemical handle space available for aminoketone synthesis.

The two substrate-scope figures also clarify why V79G receives the discovery assignment. V79G generally behaved faster in the core amino-acid subset and showed 2.7–57.5-fold improvement in catalytic efficiency relative to wild type, while V79A gave 2.4–64.8-fold improvement. These values make V79G attractive for exploring the largest number of possible aminoketone entries. They do not, however, settle the preparative question because a useful preparative catalyst must also remain active under the selected process temperature and must accept economical thioester surrogates.

Table 3. Functional interpretation of the principal *Thermus thermophilus* α-oxoamine synthase V79 variants under the TSLP method.

Variant	Dominant strength	Limiting factor	Assigned role
WT	Stable reference catalyst for the native and core amino-acid envelope	Limited expansion and no useful acetyl-SNAc activity under the tested combinations	Comparator for defining the minimum process envelope
V79A	Broad amino-acid activity, strongest severe-temperature persistence and successful acetyl-SNAc pyrrole cascade	Slightly less exploratory than V79G in the activity screen	Preparative catalyst for thermally assisted SNAc-based pyrrole synthesis
V79G	Broad amino-acid activity and generally rapid core-substrate behaviour	Major activity loss after severe heating at 90 °C	Discovery catalyst for identifying expanded amino-acid and acyl-donor entries
V79S	Distinct L-Pra compatibility across C2–C8 acyl-CoA donors and useful benzoyl-CoA entries	Moderate rather than dominant thermal persistence	Mapping catalyst for alkyne-bearing aminoketone and aryl/chain donor exploration
V79L	High 70 °C residual activity and conservative hydrophobic substitution	Poor persistence under the 90 °C severe-treatment field	Mechanistic comparator for hydrophobic-loop tolerance

Table 3 contains the next integration result: it provides an alternative approach and transforms screening data into catalyst roles instead of just giving the order of activity. Wild-type remains a reference, V79G - exploratory, V79A - preperative, V79S - special chemical mapping variant, V79L - mechanistic comparing. Table 3 provides an answer to the first sub-question raised earlier as well: differentiation is possible with one and the same dataset if we consider each individual role of the enzyme.

3.3 Acyl-donor elasticity allows route-mapping

An additional value of the acyl-donor layer can be mentioned. As expected, V79G, V79A and V79S kept catalytic activity towards all C2–C8 acyl-CoAs tested. Thus, substitution of the wild-type residue in position V79 does not prevent recognition of acyl-thioesters necessary for production of short- and medium-chain aminoketones. Furthermore, V79G was able to extend this range to C10 and C12 acyl-CoAs with core amino acids and showed low level of benzoyl-CoA condensation with Gly and L-Ala. Therefore, V79G variant is valuable in case if it is necessary to check donor space hydrophobicity or aryl groups prior to choosing a better preparation catalyst.

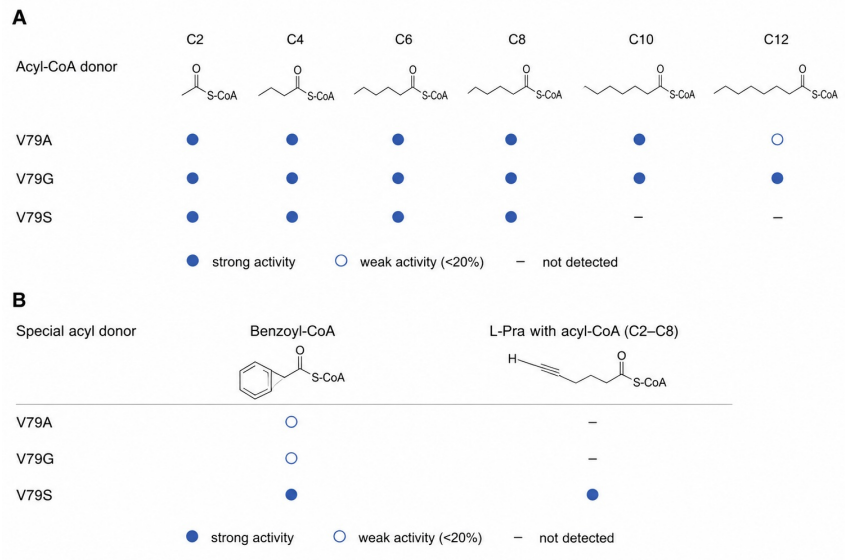

Figure 8. Acyl-donor activity map used to define the elasticity term in the TSLP model. V79A, V79G and V79S retain broad C2–C8 acyl-CoA compatibility, V79G extends to longer C10–C12 donors, and V79S provides strong activity for selected special-donor combinations.

As regards V79S variant, it possesses another route mapping ability. Namely, V79S shows activity towards C2–C8 acyl-CoAs with L-Pra donor. The fact is of great interest, since this variant allows introduction of a propargyl group into the final product of aminoketones family. Propargyl compounds are very versatile as far as further modifications are concerned, e.g. click-type reactions, surface conjugations, modular nitrogen-containing material synthesis. The fact that V79S is active with L-Ala, Gly, L-Ser and L-Cpg with benzoyl-CoA proves that V79S has changed recognition mechanism.

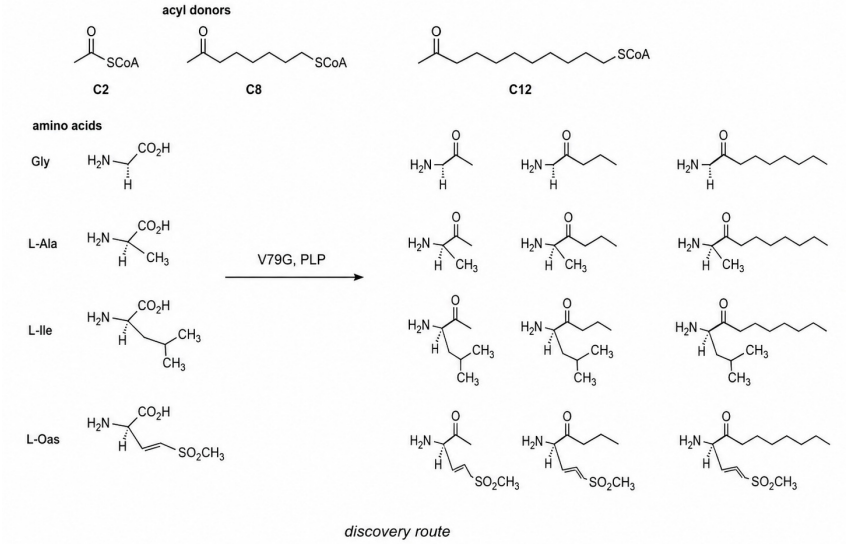

Figure 9. Discovery-route matrix connecting representative amino acids with C2, C8 and C12 acyl donors. The scheme shows how the engineered V79G/PLP catalyst generates a family of aminoketones from natural and unnatural amino acids, supporting the assignment of V79G as the preferred exploratory variant.

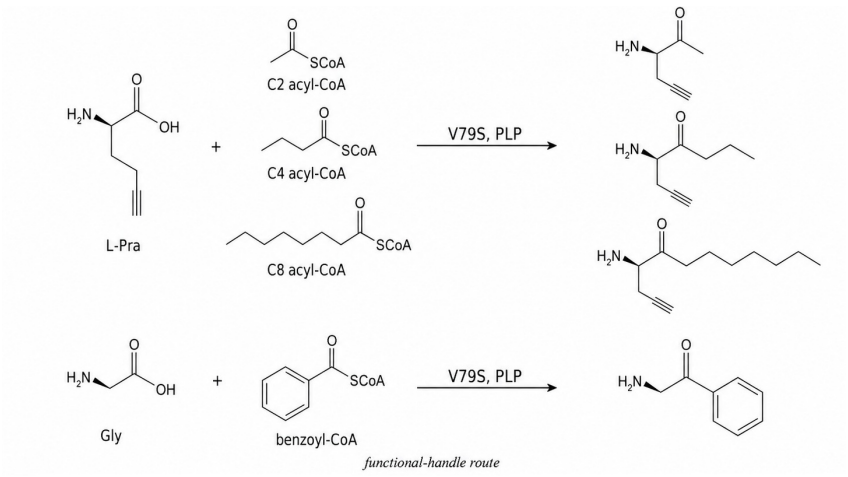

Figure 10. Functional-handle route enabled by V79S/PLP. L-Pra is condensed with C2, C4 and C8 acyl-CoA donors to produce alkyne-bearing aminoketones, and Gly is condensed with benzoyl-CoA to access an aryl aminoketone. These transformations explain why V79S is assigned to propargyl and aryl-donor mapping within the TSLP output.

Figures 8–10 convert the acyl-donor screen into route logic. The activity map is the evidence layer, the discovery matrix is the broad-product-family layer, and the functional-handle route is the specialty-product layer. Their combined interpretation shows that V79G and V79S are not redundant. V79G is best for mapping donor reach, while V79S is best for targeted functional-handle chemistry.

3.4 Thermostability changes the preparative ranking

Thermal persistence is the main reason the final process ranking differs from the activity-screen ranking. V79G performs strongly as an exploratory variant, but its residual activity falls to 56% after two hours at 70 °C and to approximately 5% or less after prolonged 90 °C treatment. V79A retains 78% activity after two hours at 70 °C and approximately 60%

activity after the severe 90 °C treatment. V79S retains 79% at 70 °C and about 45% after the 90 °C test. These values establish V79A as the most robust preparative candidate among the active engineered variants.

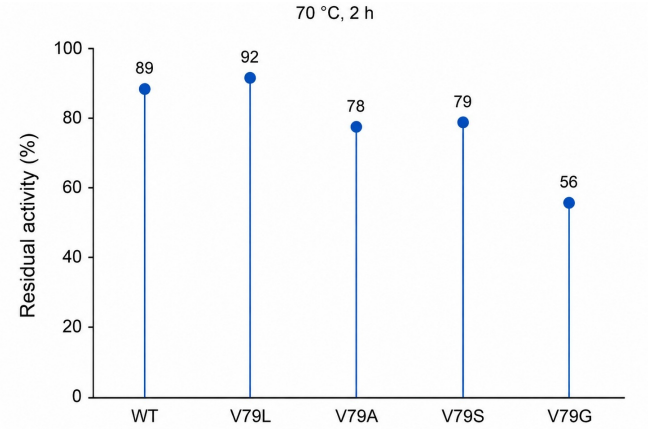

Figure 11. Residual activity after heat treatment at 70 °C for 2 h. WT, V79L, V79A and V79S retain high activity, while V79G shows a lower but still substantial residual activity. This field confirms thermal competence but does not fully resolve preparative priority.

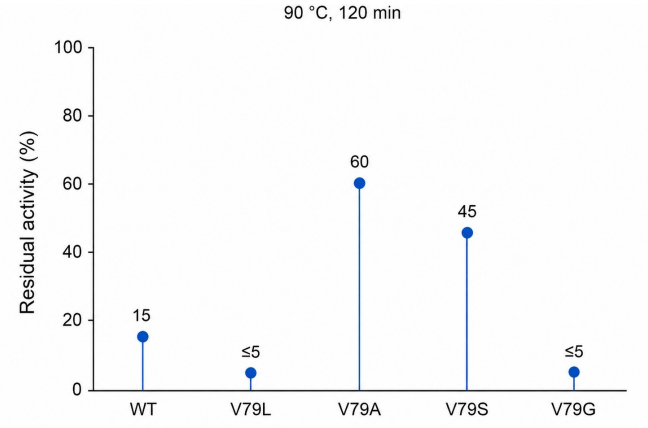

Figure 12. Residual activity after severe heat treatment at 90 °C for 120 min. V79A retains about 60% activity, V79S about 45%, WT about 15%, and V79L/V79G about 5% or less. This field distinguishes V79A as the strongest preparative variant under high-temperature stress.

Figures 11 and 12 show how the extent of heat treatment is important. For 70 °C, there are still several active catalysts, and thus the figure proves the thermal suitability of the enzyme family. For 90 °C, the separation occurs clearly, and V79A stands out as the preparative catalyst of choice. More importantly, this shows that the thermostability is not simply decoration, but a property that influences the recommendation of the catalyst.

The thermal information also precludes an erroneous interpretation of the process. The mere fact that a catalyst withstands harsh heat treatment does not imply that it will function best under harsh conditions. As explained above, the useful pyrrole was formed in the SNAc cascade already at 60 °C. Thus, the heat data provide evidence for process robustness, and do not imply that all syntheses should be done at the maximum 90 °C. This is an important aspect when choosing the optimum conditions as it depends on the enzyme stability, thioester reactivity, aminoketone production, chemical reaction and product stability.

3.5 The process capability relies on the compatibility with SNAc

This compatibility is the most essential preparative feature as it allows the replacement of expensive acyl-CoA donors with much simpler SNAc molecules. Acyl-CoA is an efficient substrate but requires additional process steps due to its high price and possible recyclability issues. SNAc thioesters are not only cheaper but also easier to handle. Their disadvantage consists in removal of many CoA interactions, meaning that the process ability with SNAc is a more stringent condition than activity with CoA alone. The wild-type *Thermus thermophilus* α-oxoamine synthase showed no acetyl-SNAc activity at the tested conditions. Instead, three mutants were observed to produce products from acetyl-SNAc with some amino acids. Most impressively, V79A, glycine, acetyl-SNAc and methyl acetoacetate provided for a preparatively significant

35% analytical yield of pyrrole 1.

The 35% yield is not intended to represent the optimal preparative yield in any way. Its significance lies in the fact that the mutant provides for the proof-of-concept for a simplified SNAc process scheme, which lacks a CoA recycling module. This can be seen from the fact that the yield increase was negligible when the acetyl-SNAc concentration rose from 32 to 800 mM. This implies that the process was not limited by the thioester donor concentration at least when both enzyme and substrate are present. Other possibilities would include the analysis of enzyme concentration, residence time, water activity, product isolation and methyl acetoacetate capture rate.

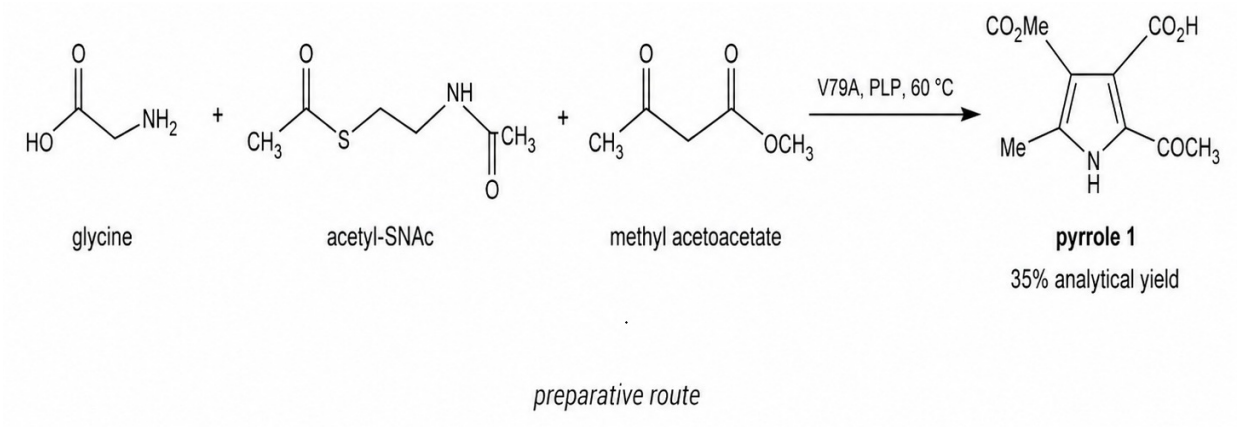

Figure 13. Preparative SNAc route to pyrrole 1. Glycine, acetyl-SNAc and methyl acetoacetate are coupled through V79A/PLP at 60 °C to furnish the substituted pyrrole in 35% analytical yield. This route provides the strongest evidence for assigning V79A to simplified thioester-based preparative synthesis.

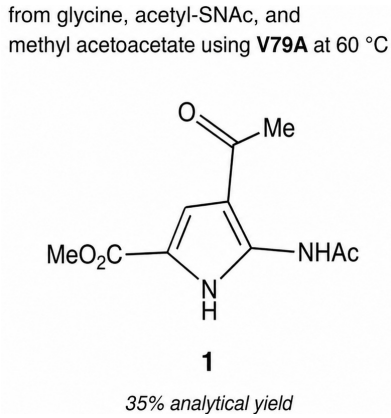

Figure 14. Product-focused view of pyrrole 1 generated from glycine, acetyl-SNAc and methyl acetoacetate using V79A at 60 °C. The 35% analytical yield is used as the SNAc-cascade utility field in the process-readiness score.

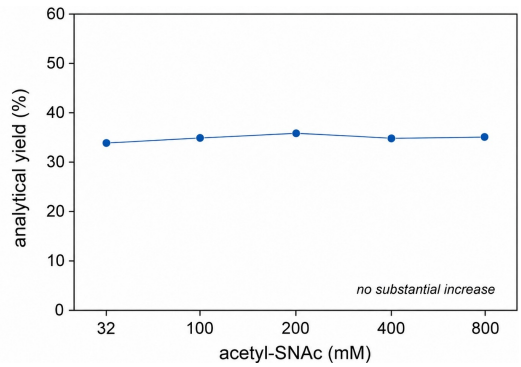

Figure 15. Effect of acetyl-SNAc loading on analytical pyrrole yield. The response remains close to 35% over 32–800 mM acetyl-SNAc, indicating that additional thioester alone is not sufficient to improve the cascade and that further optimization should target the full reaction environment.

Figures 13–15 are the decisive evidence for assigning V79A to preparation. The route scheme defines the chemical transformation, the compact cascade shows the three-component coupling logic, the product panel fixes the analytical yield, and the loading-response figure rules out a simple excess-donor solution. Together, the figures answer the economic part of the research question: the useful preparative variant is the one that enables a simplified thioester cascade under thermally tolerant conditions, not the one that merely shows the widest activity screen.

3.6 Integrated route recommendations and mechanistic interpretation

Table 4. Route recommendations generated by thermokinetic substrate-lattice prioritization.

Synthetic objective	Recommended variant	Justification
Amino-acid discovery across natural and unnatural entries	V79G	Strong exploratory breadth and generally rapid activity in the core amino-acid subset make this variant the preferred first-pass screening catalyst.
Preparative pyrrole synthesis with acetyl-SNAc	V79A	The variant combines broad activity, approximately 60% residual activity after severe 90 °C treatment and a demonstrated 35% analytical pyrrole yield at 60 °C.
Alkyne-bearing aminoketone access	V79S	L-Pra condensation with C2–C8 acyl-CoA donors provides an entry to propargylated products suitable for subsequent functionalization.
Hydrophobic acyl-chain exploration	V79G, followed by V79A validation	V79G extends activity to C10 and C12 acyl-CoA donors; V79A should be used for validation when thermal robustness becomes a process requirement.
Aryl-donor mapping	V79S and V79G	V79S supports benzoyl-CoA combinations with L-Ala, Gly, L-Ser and L-Cpg, while V79G shows slow Gly/L-Ala benzoyl-CoA condensation.

Table 4 is the definitive solution to the paper's research problem: the conversion of the experimental dataset into a route-selection map is only possible through a differentiation of the variants according to their synthetic objective. V79G provides extra flexibility in exploring potential reactions, V79S matches specific functionalized aminoketone chemistry and V79A gives the strongest SNAc-assisted route to the production of pyrroles. Therefore, the answer provided here goes beyond a general observation about increased catalytic activity upon V79 engineering.

Chemically speaking, route selection based on the analysis of the results above appears to be quite rational, since it takes into account the conformational properties of residue 79. Removal of side-chain volume in glycine facilitates exploration but decreases stability at severe temperatures. Conversely, alanine imposes slightly smaller demands on volume but retains a methyl group that could help maintain local packing and hence explains higher severe temperature activity. Polar serine adds polarity without changing local volume, which may impact hydrogen bonding or solvent interactions and thereby leads to a unique propargyl/benzoyl chemistry mapping pattern. Overall, it is clear that TSLP result is not purely numerical but structurally relevant in explaining pocket opening, packing stabilization and local polarity.

3.7 Materials relevance, limitations and future optimization

Relevance of the current research lies in the ability of the developed selection model to produce nitrogen-containing building blocks under environmentally-conscious conditions. A route selection model, identifying the required donor for each catalytically enabled transformation of interest, enables focusing on the development of the promising variant(s). This means that the current study is in accordance with the goals of a technology-and-materials journal since it develops an approach towards more sustainable manufacturing processes.

At the same time, there are several limitations to be recognized. First of all, TSLP is based on currently available categorical and activity data and cannot serve as a substitute to a kinetic modelling or optimization of yields in isolated enzyme experiments. The 35% analytically identified pyrrole yield is very promising, but still far from a conclusive target value. In addition, the absence of increased yield at elevated acetyl-SNAc concentration highlights the necessity to optimize the entire reaction medium rather than the individual components. As the next steps, the following optimizations are suggested: quantification of additional donors' kinetics, testing enzyme immobilization, studying solvent and pH tolerances and implementation of continuous flow reactors in pyrrole synthesis involving β-keto ester partners other than those used here.

4 Conclusions

In response to the research question asked by this work, the activity spectrum, thermostability and SNAc-cascade results of the mutant variants *Thermus thermophilus* α-oxoamine synthase V79 can be mapped to reveal a practical selection of

catalyst roles. However, the appropriate answer does not involve ranking all mutants. Rather, it involves designating V79G for discovery and general screening, V79S for propargyl and select aryl-CoA acceptors, and V79A as the top preparative catalyst. This result follows from the integrated analysis of amino acid acceptor breadth, acyl-donor tolerance, high-temperature activity retention and thioester cascade function. As a scientific finding, the separation of exploratory value and preparative suitability is key. The mutant variant G79 is a fast and broad screening catalyst, but its thermostability is too low for it to be the optimal preparative catalyst at elevated temperature. V79S is neither the fastest nor most thermostable mutant. Yet it has unique chemical value as a catalyst for L-Pra and selected benzoyl-CoA derivatives. V79A is clearly the most promising preparative variant, combining acceptable amino acid breadth, substantial thermostability and proof-of-concept preparation of pyrrole via the glycine, acetyl-SNAc and methyl acetoacetate pathway at 60 °C in 35% yield. Thus, TSLP represents a novel methodology for assigning roles to biocatalysts based on screening and discovery information. Specifically, it suggests using V79A for thermally-optimized SNAc-catalyzed synthesis of aminoketones and heterocycles, with V79S and V79G for initial discovery and handle expansion. Future work will extend from simple lattice scoring to precise kinetic evaluation, isolated yields and more advanced reaction setups, such as catalyst immobilization, comparative donor recyclability and continuous flow reactors.

Conflict of Interest

The author declares no conflict of interest.

Data Availability

The input values used for route selection are the amino-acid activity, acyl-donor acceptance, residual-activity and SNAc-cascade yield values cited in the Materials and Methodology section. The figure assets in the project directory document the structural, substrate-scope, thermal and cascade fields used to explain the TSLP ranking. No separate dataset is required to reproduce the qualitative catalyst-role assignment described here.

References

[1] Sheldon, R. A.; Woodley, J. M. Role of biocatalysis in sustainable chemistry. *Chemical Reviews* 2018, *118*, 801–838. https://doi.org/10.1021/acs.chemrev.7b00203.

[2] Bornscheuer, U. T.; Huisman, G. W.; Kazlauskas, R. J.; Lutz, S.; Moore, J. C.; Robins, K. Engineering the third wave of biocatalysis. *Nature* 2012, *485*, 185–194.

[3] Hauer, B. Embracing nature's catalysts: a viewpoint on the future of biocatalysis. *ACS Catalysis* 2020, *10*, 8418–8427.

[4] Reetz, M. T. Biocatalysis in organic chemistry and biotechnology: past, present, and future. *Journal of the American Chemical Society* 2013, *135*, 12480–12496.

[5] Devine, P. N.; Howard, R. M.; Kumar, R.; Thompson, M. P.; Truppo, M. D.; Turner, N. J. Extending the application of biocatalysis to meet the challenges of drug development. *Nature Reviews Chemistry* 2018, *2*, 409–421.

[6] Truppo, M. D. Biocatalysis in the pharmaceutical industry: the need for speed. *ACS Medicinal Chemistry Letters* 2017, *8*, 476–480.

[7] Arnold, F. H. Directed evolution: bringing new chemistry to life. *Angewandte Chemie International Edition* 2018, *57*, 4143–4148.

[8] Turner, N. J. Directed evolution drives the next generation of biocatalysts. *Nature Chemical Biology* 2009, *5*, 567–573.

[9] Zeymer, C.; Hilvert, D. Directed evolution of protein catalysts. *Annual Review of Biochemistry* 2018, *87*, 131–157.

[10] Denard, C. A.; Ren, H.; Zhao, H. Improving and repurposing biocatalysts via directed evolution. *Current Opinion in Chemical Biology* 2015, *25*, 55–64.

[11] Turner, N. J.; O'Reilly, E. Biocatalytic retrosynthesis. *Nature Chemical Biology* 2013, *9*, 285–288. https://doi.org/10.1038/nchembio.1235.

[12] de Souza, R. O. M. A.; Miranda, L. S. M.; Bornscheuer, U. T. A retrosynthesis approach for biocatalysis in organic synthesis. *Chemistry–A European Journal* 2017, *23*, 12040–12063. https://doi.org/10.1002/chem.201702235.

[13] Finnigan, W.; Hepworth, L. J.; Flitsch, S. L.; Turner, N. J. RetroBioCat as a computer-aided synthesis planning tool for biocatalytic reactions and cascades. *Nature Catalysis* 2021, *4*, 98–104. https://doi.org/10.1038/s41929-020-00556-z.

[14] France, S. P.; Hepworth, L. J.; Turner, N. J.; Flitsch, S. L. Constructing biocatalytic cascades: in vitro and in vivo approaches to de novo multi-enzyme pathways. *ACS Catalysis* 2017, *7*, 710–724. https://doi.org/10.1021/acscatal.6b02979.

[15] Huffman, M. A.; Fryszkowska, A.; Alvizo, O.; Borra-Garske, M.; Campos, K. R.; Canada, K. A.; Devine, P. N.; Duan, D.; Forstater, J. H.; Grosser, S. T.; et al. Design of an in vitro biocatalytic cascade for the manufacture of islatravir. *Science* 2019, *366*, 1255–1259. https://doi.org/10.1126/science.aay8484.

[16] Eliot, A. C.; Kirsch, J. F. Pyridoxal phosphate enzymes: mechanistic, structural, and evolutionary considerations. *Annual Review of Biochemistry* 2004, *73*, 383–415.

[17] Toney, M. D. Controlling reaction specificity in pyridoxal phosphate enzymes. *Biochimica et Biophysica Acta* 2011, *1814*, 1407–1418.

[18] Dunathan, H. C. Conformation and reaction specificity in pyridoxal phosphate enzymes. *Proceedings of the National Academy of Sciences of the United States of America* 1966, *55*, 712–716.

[19] Percudani, R.; Peracchi, A. A genomic overview of pyridoxal-phosphate-dependent enzymes. *EMBO Reports* 2003, *4*, 850–854.

[20] Schneider, G.; Käck, H.; Lindqvist, Y. The manifold of vitamin B6 dependent enzymes. *Structure* 2000, *8*, R1–R6.

[21] Christen, P.; Mehta, P. K. From cofactor to enzymes: the molecular evolution of pyridoxal-5'-phosphate-dependent enzymes. *Chemical Record* 2001, *1*, 436–447.

[22] Cane, D. E.; Walsh, C. T.; Khosla, C. Harnessing the biosynthetic code: combinations, permutations, and mutations. *Science* 1998, *282*, 63–68.

[23] Hunter, G. A.; Ferreira, G. C. Molecular enzymology of 5-aminolevulinate synthase, the gatekeeper of heme biosynthesis. *Biochimica et Biophysica Acta* 2011, *1814*, 1467–1473.

[24] Alexeev, D.; Alexeeva, M.; Baxter, R. L.; Campopiano, D. J.; Webster, S. P.; Sawyer, L. The crystal structure of 8-amino-7-oxononanoate synthase: a bacterial PLP-dependent, acyl-CoA-condensing enzyme. *Journal of Molecular Biology* 1998, *284*, 401–419.

[25] Yard, B. A.; Carter, L. G.; Johnson, K. A.; Overton, I. M.; Dorward, M.; Liu, H.; McMahon, S. A.; Oke, M.; Puech, D.; Barton, G. J.; Naismith, J. H.; Campopiano, D. J. The structure of serine palmitoyltransferase: gateway to sphingolipid biosynthesis. *Journal of Molecular Biology* 2007, *370*, 870–886.

[26] Lowther, J.; Yard, B. A.; Johnson, K. A.; Carter, L. G.; Bhat, V. T.; Raman, M. C. C.; Clarke, D. J.; Ramakers, B.; McMahon, S. A.; Naismith, J. H.; Campopiano, D. J. Inhibition of serine palmitoyltransferase by L-penicillamine and structural insights into PLP-dependent aminothiol chemistry. *Biochemical Journal* 2010, *431*, 321–331.

[27] Ashley, B.; Baslé, A.; Sajjad, M.; El Ashram, A.; Kelis, P.; Marles-Wright, J.; Campopiano, D. J. Versatile chemo-biocatalytic cascade driven by a thermophilic and irreversible C–C bond-forming α-oxoamine synthase. *ACS Sustainable Chemistry & Engineering* 2023, *11*, 7997–8002. https://doi.org/10.1021/acssuschemeng.3c00243.

[28] Knorr, L. Synthese von Pyrrolderivaten. *Berichte der Deutschen Chemischen Gesellschaft* 1884, *17*, 1635–1642.

[29] Estévez, V.; Villacampa, M.; Menéndez, J. C. Recent advances in the synthesis of pyrroles by multicomponent reactions. *Chemical Society Reviews* 2010, *39*, 4402–4421.

[30] Ashley, B.; Mathew, S.; Sajjad, M.; Zhu, Y.; Novikovs, N.; Baslé, A.; Marles-Wright, J.; Campopiano, D. J. Rational engineering of a thermostable α-oxoamine synthase biocatalyst expands the substrate scope and synthetic applicability. *Communications Chemistry* 2025, *8*, 78. https://doi.org/10.1038/s42004-025-01448-8.